

D. Paul<sup>1</sup>, and M. Zaitsev<sup>1</sup>

<sup>1</sup>Department for Diagnostic Radiology, Medical Physics, University Hospital Freiburg, Freiburg, Germany

## Introduction

bSSFP sequences (aka TrueFISP or FIESTA) have found widespread application in clinical MR imaging (e.g. cardiac and abdominal imaging) due to their high SNR efficiency. In order to obtain banding artifact free images repetition times (TR) as short as few milliseconds are necessary. In combination with high flip angles (on the order of 50 to 70°) this often leads to SAR-problems especially at high field strengths as 3 T and above.

To overcome this limitations, variable flip angle schemes were introduced in bSSFP imaging [1,2]. The aim of this work was to investigate the resolution and

SNR properties of bSSFP with variable flip angles.

## Method

The flip angles were varied over k-space such that outer k-space lines were sampled using a smaller flip angle  $\alpha_{\min}$  while central part of k-space was acquired using high flip angles  $\alpha_{\max}$ . The flip angle  $\alpha_{\max}$  was chosen as the maximum allowed flip angle derived from an abdominal measurement in a healthy volunteer and was not changed in subsequent phantom experiments. The transition between the two flip angles was realized in  $M$  steps using a trigonometric function [2] (see Fig. 1). For preparation  $\alpha/2$ -pulse was used. Multiple variants with different values for  $\alpha_{\min}$ ,  $\alpha_{\max}$ , and  $M$  were taken into account. In addition, a TrueFISP sequence with constant flip angle was used.

In order to investigate the resolution properties of the different variants, images of a resolution phantom with raster structures (aligned in PE direction) were acquired at 3 T (Magnetom Trio, Siemens Medical Solutions, Erlangen, Germany). The PSF was simulated using Matlab (The MathWorks, Natick, Massachusetts, USA) for the different sequence variants and tissue types (e.g. liver, kidney).

For SNR evaluation abdominal images of healthy volunteers were acquired. SNR was evaluated quantitatively in a ROI analysis as the mean signal intensity in homogenous media divided by the standard deviation of the noise outside the volunteer.

## Results

Figure 1b shows the maximum flip angle for the center of k-space plotted against ramp length  $M$ . Using  $\alpha_{\min} = 1^\circ$  the flip angle  $\alpha_{\max}$  can be increased up to 47°,  $\alpha_{\min}=20^\circ$  resulted in  $\alpha_{\max}=42^\circ$ , respectively. In comparison, standard TrueFISP with constant flip angles allows  $\alpha=34^\circ$  due to SAR limitations.

The usage of smaller flip angles for outer parts of k-space results in lower signal intensity and thus affects the image resolution. The Full Width at Half Maximum (FWHM) of the simulated PSF (simulated and plotted in fig 2 for liver tissue) increase with ramp length  $M$ . While for standard TrueFISP FWHM=0.96 it increases up to FWHM=1.09 using  $\alpha_{\min}=20^\circ$ , using  $\alpha_{\min}=1^\circ$  results in FWHM=1.42, respectively.

This effect may be observed when imaging small structures like the phantom raster (see Fig. 3a). Despite of the PSF broadening the signal intensity  $\Delta S$  of the raster structure increases with  $\alpha_{\max}$ . It is to be noted, however, that the signal in the surrounding areas (bulk water) inside the phantom experiences much stronger increase, as seen from Fig. 3b.

The influence of flip angle variation on SNR is shown in Fig. 4. The SNR of liver and kidney from a healthy volunteer, as well as the CNR (difference of SNR values) increase with ramp length  $M$ . Using the variable flip angle approach, SNR increase of up to 35% can be achieved. CNR between liver and kidney (as shown as red line in Fig. 4) increases as well.

## Discussion

Flip angle variations provide a useful tool in order to overcome SAR limitations and increase SNR (and CNR). Using higher flip angles for central k-space parts results in a substantial higher SNR. The influence of flip angle variations on the in-plane resolution should not be underestimated: the variation scheme acts like a k-space filter, broadening small structures. However, due to the fact that resolution in MRI is often SNR-limited, the gain at SNR due to the use of higher flip angles overcompensates the broadening introduced.

For abdominal imaging, where an additional k-space filter is often used to reduce ringing artifacts, variable flip angles can be used to increases SNR while simultaneously act as the k-space filter.

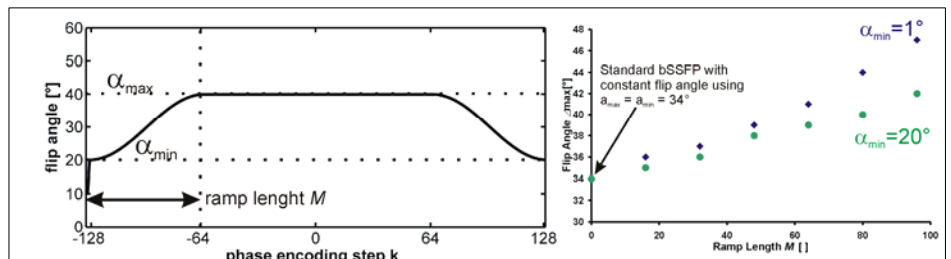


**Fig. 1a:** Flip angle scheme over k-space (256 PE steps) using  $\alpha_{\min}=20^\circ$ ,  $\alpha_{\max}=40^\circ$  and  $M=64$ .  $\alpha/2$ -Preparation was performed prior to the data acquisition.

**Fig. 1b:** Flip angle  $\alpha_{\max}$  for the k-space center depending on  $\alpha_{\min}$  and ramp length  $M$ .

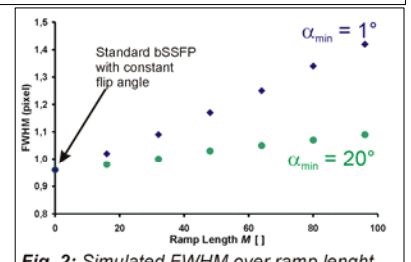


**Fig. 2:** Simulated FWHM over ramp length  $M$  for  $\alpha_{\min}=20^\circ$  and  $\alpha_{\min}=1^\circ$ . FWHM increases with the ramp length.

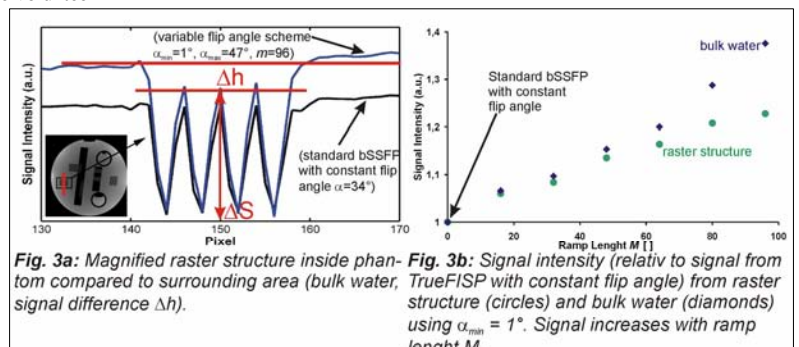


**Fig. 3a:** Magnified raster structure inside phantom. **Fig. 3b:** Signal intensity (relative to signal from tom compared to surrounding area (bulk water, TrueFISP with constant flip angle) from raster structure (circles) and bulk water (diamonds) using  $\alpha_{\min}=1^\circ$ . Signal increases with ramp length  $M$ .

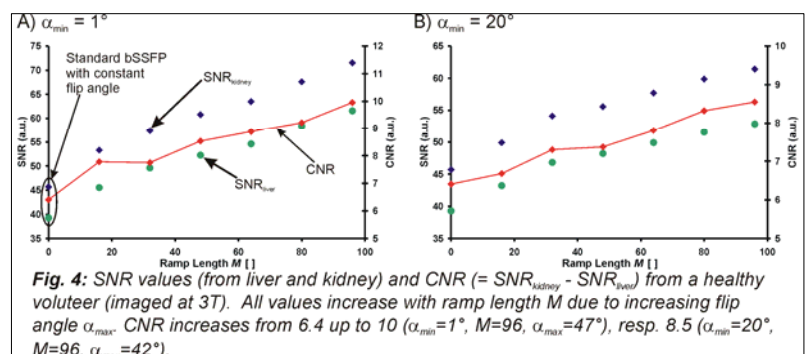


**Fig. 4:** SNR values (from liver and kidney) and CNR (=  $SNR_{\text{kidney}} - SNR_{\text{liver}}$ ) from a healthy volunteer (imaged at 3T). All values increase with ramp length  $M$  due to increasing flip angle  $\alpha_{\max}$ . CNR increases from 6.4 up to 10 ( $\alpha_{\min}=1^\circ$ ,  $M=96$ ,  $\alpha_{\max}=47^\circ$ ), resp. 8.5 ( $\alpha_{\min}=20^\circ$ ,  $M=96$ ,  $\alpha_{\max}=42^\circ$ ).